

---

# CMS Physics Analysis Summary

---

Contact: cms-phys-conveners-ftr@cern.ch

2018/12/11

## Predictions on the precision achievable for small system flow observables in the context of the HL-LHC

The CMS Collaboration

### Abstract

In this note, we discuss how the future HL-LHC program will enable highly precise measurements of flow observables in small systems. Projections of the statistical uncertainties achievable for symmetric cumulant analyses at  $\sqrt{s} = 13$  TeV for pp collisions and at  $\sqrt{s_{NN}} = 5.02$  TeV for pPb collisions are presented. The improvement in the symmetric cumulant precision by increasing the pp beam energy to 14 TeV, while extending the CMS tracker pseudorapidity coverage to  $|\eta| < 4$ , is also shown. In addition, we show how the HL-LHC will allow for elliptic flow measurements of  $D^0$  and  $J/\psi$  mesons in 8.16 TeV pPb collisions that are a factor of two more precise than currently possible.



## 1 Introduction

In heavy ion collisions, a quark-gluon plasma (QGP) state is created in the overlap region of the colliding ions. The hydrodynamic expansion of the QGP is reflected in the observed correlations of particles in the final state. These correlations are usually quantified by the Fourier harmonic coefficients ( $v_n$ ) of the final-state particle azimuthal distributions. A key feature of such correlations in ultra-relativistic nucleus-nucleus collisions is a pronounced structure on the near side (relative azimuthal angle  $|\Delta\phi| \approx 0$ ) that extends over a large range in relative pseudorapidity ( $|\Delta\eta|$  up to 4 units or more). This feature is known as the “ridge” and is thought to be a consequence of the QGP medium reflecting higher-order terms in the overlap geometry of the collision (see, e.g., Ref. [1]). However, a ridge-like behavior has also been found at the LHC in high multiplicity events for small colliding systems, such as the pp and pPb systems. The collective nature of this correlation across all colliding systems may challenge the current accepted paradigm that describes both small and large colliding systems within a similar QCD framework. Despite a significant effort by the CMS, ATLAS, and ALICE experiments at the LHC to explore the ridge, its origin is still unknown. With the HL-LHC program, it will be possible to reach an unprecedented multiplicity regime and an experimental precision that will help to establish the origin of the ridge correlations in small systems. In this note, projections for the key observables of symmetric cumulant correlations and  $v_2$  coefficients of heavy-flavor particles are presented for pp collisions at 13 and 14 TeV. In addition, projections for a future pPb run are provided. All of the projections are based on current CMS results presented in Refs. [2–5] and assume similar tracking performance and trigger efficiencies as found for these earlier analyses. It is also assumed that the data taking conditions will be similar, other than for the extended rapidity coverage of the CMS tracker that will be available with the HL-LHC.

## 2 Upgraded CMS Detector

The CMS detector [6] will be substantially upgraded in order to fully exploit the physics potential offered by the increase in luminosity, and to cope with the demanding operational conditions at the HL-LHC [7–11]. The upgrade of the first level hardware trigger (L1) will allow for an increase of L1 rate and latency to about 750 kHz and 12.5  $\mu$ s, respectively, and the high-level software trigger (HLT) is expected to reduce the rate by about a factor of 100, to 7.5 kHz. The entire pixel and strip tracker detectors will be replaced to increase the granularity, reduce the material budget in the tracking volume, improve the radiation hardness, and extend the geometrical coverage and provide efficient tracking up to pseudorapidities of about  $|\eta| = 4$ . The muon system will be enhanced by upgrading the electronics of the existing cathode strip chambers (CSC), resistive plate chambers (RPC) and drift tubes (DT). New muon detectors based on improved RPC and gas electron multiplier (GEM) technologies will be installed to add redundancy, increase the geometrical coverage up to about  $|\eta| = 2.8$ , and improve the trigger and reconstruction performance in the forward region. The barrel electromagnetic calorimeter (ECAL) will feature the upgraded front-end electronics that will be able to exploit the information from single crystals at the L1 trigger level, to accommodate trigger latency and bandwidth requirements, and to provide 160 MHz sampling allowing high precision timing capability for photons. The hadronic calorimeter (HCAL), consisting in the barrel region of brass absorber plates and plastic scintillator layers, will be read out by silicon photomultipliers (SiPMs). The endcap electromagnetic and hadron calorimeters will be replaced with a new combined sampling calorimeter (HGCal) that will provide highly-segmented spatial information in both transverse and longitudinal directions, as well as high-precision timing information. Finally, the addition of a new timing detector for minimum ionizing particles (MTD) in

both barrel and endcap regions is envisaged to provide the capability for 4-dimensional reconstruction of interaction vertices that will significantly offset the CMS performance degradation due to high pileup rates.

A detailed overview of the CMS detector upgrade program is presented in Ref. [7–11], while the expected performance of the reconstruction algorithms and pileup mitigation with the CMS detector is summarised in Ref. [12].

### 3 Projection for Symmetric Cumulants

The symmetric cumulants, denoted  $SC(m, n)$ , are based on 4-particle correlations and measure correlations between the Fourier coefficients  $m$  and  $n$ . In this section, the improvement in statistical precision for these measurements that is achieved by increasing the center-of-mass energy and by extending the CMS tracker rapidity coverage is considered for pp collisions. The impact of increasing the integrated luminosity on the statistical precision of pPb symmetric cumulant results is also studied.

#### 3.1 HL-LHC projections for 13 TeV pp collisions and for 5.02 TeV pPb collisions

In Fig. 1, the projection for the symmetric cumulant measurement  $SC(2,3)$  are shown for pp collisions 13 TeV and pPb collisions at 5.02 TeV. The data points are the CMS results using Run 1 and Run 2 data and are found using the 4-particle cumulant method. Only statistical errors are displayed. The results are expressed as a function of the total multiplicity, as corrected for efficiency and the experimental  $p_T$  range. The vertical dashed line shows the multiplicity range above which data were collected using a high-multiplicity trigger. The rising trend of  $SC(2,3)$  observed in data when moving toward lower multiplicities is known to come from nonflow effects. At the highest multiplicities,  $SC(2,3)$  is weakly dependent on nonflow and a high precision measurement of a negative signal will further constrain the current interpretation of the ridge phenomenon in small colliding systems.

In addition, it has been shown that nonflow effects can be reduced, at the expense of statistical precision, by analyzing the data in multiple subevent regions in the intermediate and low multiplicity ranges [4]. The experimental precision that can be achieved with the HL-LHC for the 2-, 3-, and 4-subevent methods are also shown in Fig. 1. The projections are for pp collisions at 13 TeV (left) and for pPb collisions at 5.02 TeV (right), assuming integrated luminosities of  $200 \text{ pb}^{-1}$  and  $1000 \text{ nb}^{-1}$  for the two systems, respectively. For these projections, constant mean  $SC(2,3)$  values are assumed as a function of total multiplicity, based on existing high-multiplicity measurements for the pp [13] and pPb [4] systems. These projections indicate that the subevent analyses should have absolute uncertainties on the order of  $10^{-7}$ . As the  $SC(2,3)$  value is particularly sensitive to the initial state and its fluctuations, a precision measurement of this quantity will test our understanding this early stage of the collision.

#### 3.2 HL-LHC projections for 14 TeV pp collisions

Figure 2 shows the same projections as in Fig. 1, but estimated for pp collisions at 14 TeV. The increase of the number of events for each multiplicity bin is estimated using the multiplicity distribution extrapolated using available data at various center-of-mass energies. Data from the 13 TeV pp analysis are displayed for comparison. With increasing center-of-mass energy, the multiplicity spectra get harder at high-multiplicity. This leads to a dramatic reduction in the experimental uncertainties, by at least an order of magnitude.

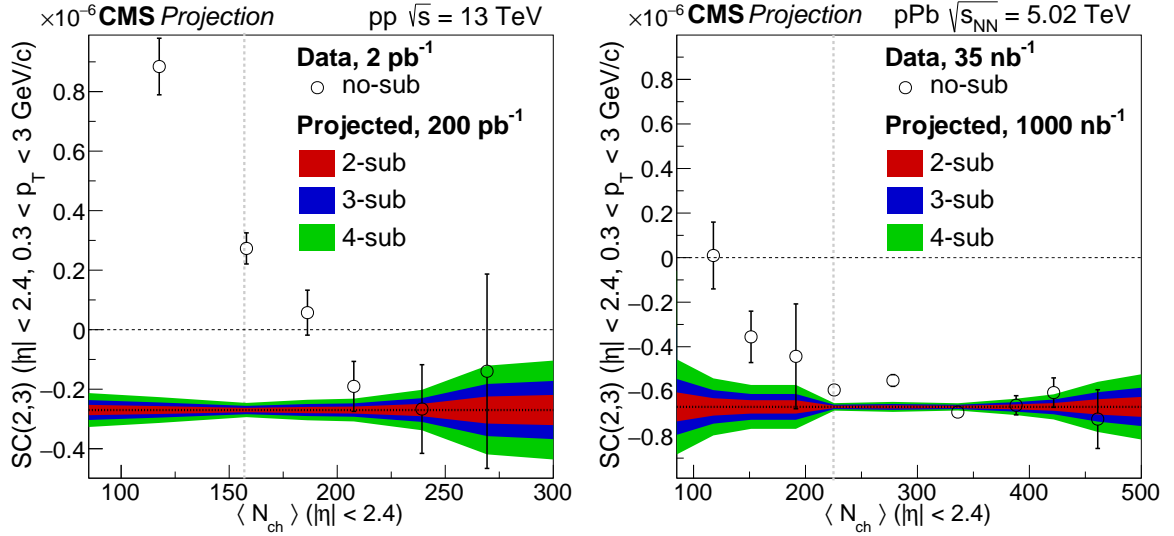


Figure 1:  $SC(2,3)$  as a function of total multiplicity in pp collisions at 13 TeV (left) and pPb collisions at 5.02 TeV (right). Only statistical uncertainties are displayed. The open circles show the current CMS results standard 4-particle cumulant method [2]. The vertical dashed line shows the multiplicity range above which data were collected using a high-multiplicity trigger. The color-shaded areas show the HL-LHC projections for 2-, 3- and 4-subevent symmetric cumulant analyses, as indicated.

### 3.3 CMS extended tracker coverage projection

For the HL-LHC runs, the CMS tracker acceptance will be extended to 4 units in pseudorapidity. The projected experimental uncertainties for pp collisions associated with this extended  $\eta$  coverage are provided in Fig. 3 based on the 3-subevent symmetric cumulant analysis. With the extended pseudorapidity range, it is no longer possible to assume a flat multiplicity distribution in  $\eta$ . Consequently, the scaling factor is calculated using Monte Carlo simulations. Pythia and EPOS are used for this simulation and found to give consistent results. The experimental uncertainties for pp collisions at both 13 and 14 TeV are found to be significantly reduced using the increased pseudorapidity coverage.

## 4 HL-LHC projections for $D^0$ and $J/\Psi$ elliptic flow

In this section, the statistical precision of elliptic flow measurement for heavy-flavor mesons with increasing integrated luminosity is studied. Figure 4 (left) shows the projections for the second Fourier harmonic coefficients as a function of  $p_T$  for  $D^0$  and  $J/\Psi$  mesons in pPb collisions at 8 TeV with integral luminosities of  $500 \text{ nb}^{-1}$  and  $2000 \text{ nb}^{-1}$ . A factor of two improvement in the experimental uncertainties is observed compared to the existing experimental results. Figure 4 (right) shows the same projections as a function of transverse kinetic energy ( $KE_T$ ) scaled by the number of constituent quarks ( $n_q$ ). The production mechanisms of open/hidden charm are poorly known. In addition, whether the charm quarks thermalize in the hot and dense environment created in high multiplicity pPb collisions is still an open question. Assuming a quark-gluon plasma production and partial thermalization of the charm quarks, the following ordering is expected at low  $KE_T$ :  $v_2(\text{charged hadrons}) > v_2(D^0) > v_2(J/\Psi)$ . With the precision made possible by the HL-LHC, it will be possible to put stringent constraints on heavy particle production and thermalization within a high multiplicity envi-

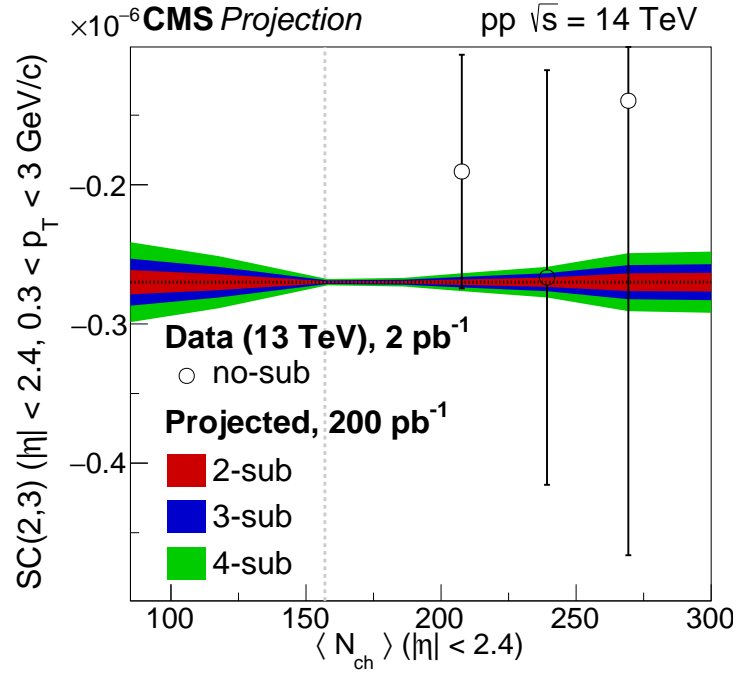


Figure 2:  $SC(2,3)$  as a function of total multiplicity in pp collisions at 14 TeV. Only statistical uncertainties are displayed. The vertical dashed line shows the multiplicity range above which data were collected using a high-multiplicity trigger. The open circles are the current CMS results at 13 TeV [2]. The color-shaded areas show the HL-LHC projections for 2-, 3- and 4-subevent symmetric cumulant analyses, as indicated.

ronment.

## 5 Summary

In this note, we have presented projections for symmetric cumulant and heavy particle elliptic flow analyses in the context of the HL-LHC. The increase of luminosity significantly reduces the experimental uncertainties compared to existing results. Such measurements will provide a better understanding of the “ridge” structure observed in small colliding system. In terms of its theoretical understanding, this is among the most controversial behaviors found in relativistic heavy-ion collisions.

## References

- [1] F. Wang, “Novel Phenomena in Particle Correlations in Relativistic Heavy-Ion Collisions”, *Prog. Part. Nucl. Phys.* **74** (2014) 35–54, doi:10.1016/j.pnpnp.2013.10.002, arXiv:1311.4444.
- [2] CMS Collaboration, “Observation of Correlated Azimuthal Anisotropy Fourier Harmonics in  $pp$  and  $p + Pb$  Collisions at the LHC”, *Phys. Rev. Lett.* **120** (2018), no. 9, 092301, doi:10.1103/PhysRevLett.120.092301, arXiv:1709.09189.

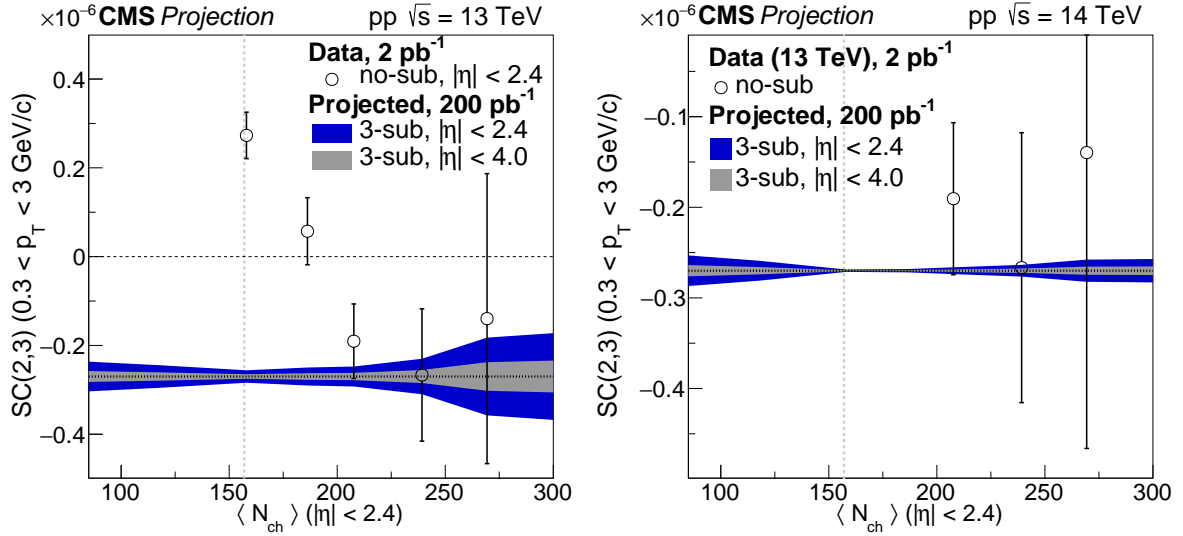


Figure 3: SC(2,3) as a function of total multiplicity in pp collisions at 13 and 14 TeV using the 3-subevent method. Only statistical uncertainties are displayed. The open circles show the current CMS results using the standard 4-particle cumulant method [2]. The vertical dashed line shows the multiplicity range above which data were collected using a high-multiplicity trigger. The blue shaded area is the projection for the current CMS tracker acceptance and the gray shaded area is the projection for CMS extended tracker acceptance.

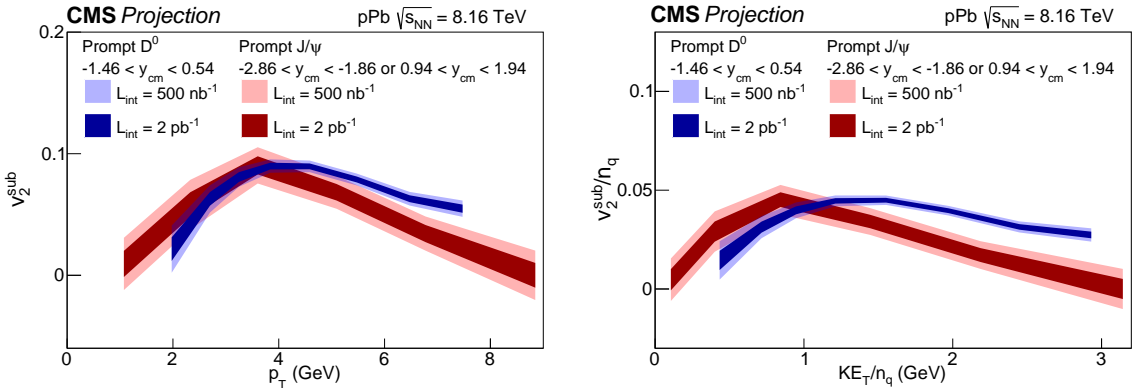


Figure 4: (Left) HL-LHC projections for  $D^0$  and  $J/\Psi$  elliptic flow as a function of  $p_T$ . (Right) Elliptic flow projections scaled by the number of constituent quarks ( $n_q$ ) as a function of the similarly scaled transverse kinetic energy ( $KE_T/n_q$ ). Only statistical uncertainties are displayed.

[3] CMS Collaboration, “Elliptic flow of charm and strange hadrons in high-multiplicity pPb collisions at  $\sqrt{s_{NN}} = 8.16$  TeV”, *Phys. Rev. Lett.* **121** (2018), no. 8, 082301, doi:10.1103/PhysRevLett.121.082301, arXiv:1804.09767.

[4] CMS Collaboration, “Measurement of correlated azimuthal anisotropy Fourier harmonics with subevent cumulants in pPb collisions at 8.16 TeV”, Technical Report CMS-PAS-HIN-18-015, CERN, Geneva, 2018.

[5] CMS Collaboration, “Observation of prompt  $J/\psi$  meson elliptic flow in high-multiplicity pPb collisions at  $\sqrt{s_{NN}} = 8.16$  TeV”, *Submitted to: Phys. Lett.* (2018) arXiv:1810.01473.

- [6] CMS Collaboration, “The CMS Experiment at the CERN LHC”, *JINST* **3** (2008) S08004, doi:10.1088/1748-0221/3/08/S08004.
- [7] CMS Collaboration, “Technical Proposal for the Phase-II Upgrade of the CMS Detector”, Technical Report CERN-LHCC-2015-010. LHCC-P-008. CMS-TDR-15-02, 2015.
- [8] CMS Collaboration, “The Phase-2 Upgrade of the CMS Tracker”, Technical Report CERN-LHCC-2017-009. CMS-TDR-014, 2017.
- [9] CMS Collaboration, “The Phase-2 Upgrade of the CMS Barrel Calorimeters Technical Design Report”, Technical Report CERN-LHCC-2017-011. CMS-TDR-015, 2017.
- [10] CMS Collaboration, “The Phase-2 Upgrade of the CMS Endcap Calorimeter”, Technical Report CERN-LHCC-2017-023. CMS-TDR-019, 2017.
- [11] CMS Collaboration, “The Phase-2 Upgrade of the CMS Muon Detectors”, Technical Report CERN-LHCC-2017-012. CMS-TDR-016, 2017.
- [12] CMS Collaboration, “CMS Phase-2 Object Performance”, CMS Physics Analysis Summary, in preparation.
- [13] ATLAS Collaboration Collaboration, “Correlated long-range mixed-harmonic fluctuations in  $pp$ ,  $p$ +Pb and low-multiplicity Pb+Pb collisions with the ATLAS detector”, Technical Report ATLAS-CONF-2018-012, CERN, Geneva, May, 2018.